

Short-pulse laser absorption in very steep plasma density gradients

Hong-bo Cai^{a)}

Institute of Applied Physics and Computational Mathematics, P.O. Box 2101, Beijing 100088, China

Wei Yu

Shanghai Institute of Optics and Fine Mechanics, Shanghai 201800, China

Shao-ping Zhu, Chun-yang Zheng, Li-hua Cao, and Bin Li

Institute of Applied Physics and Computational Mathematics, P.O. Box 8009, Beijing 100088, China

Z. Y. Chen and A. Bogerts

Department of Chemistry, University of Antwerp, B-2610 Wilrijk-Antwerp, Belgium

(Received 23 May 2006; accepted 21 August 2006; published online 15 September 2006)

An analytical fluid model for resonance absorption during the oblique incidence by femtosecond laser pulses on a small-scale-length density plasma [$k_0L \in (0.1, 10)$] is proposed. The physics of resonance absorption is analyzed more clearly as we separate the electric field into an electromagnetic part and an electrostatic part. It is found that the characteristics of the physical quantities (fractional absorption, optimum angle, etc.) in a small-scale-length plasma are quite different from the predictions of classical theory. Absorption processes are generally dependent on the density scale length. For shorter scale length or higher laser intensity, vacuum heating tends to be dominant. It is shown that the electrons being pulled out and then returned to the plasma at the interface layer by the wave field can lead to a phenomenon like wave breaking. This can lead to heating of the plasma at the expense of the wave energy. It is found that the optimum angle is independent of the laser intensity while the absorption rate increases with the laser intensity, and the absorption rate can reach as high as 25%. © 2006 American Institute of Physics.

[DOI: 10.1063/1.2354583]

The interaction of ultrashort laser pulses ($\tau_p < 1$ ps) with solid targets has become an important field of study because of many applications, such as the fast ignition scheme of inertia confinement fusion,¹ the plasma-based particle accelerator,² coherent x/γ -ray sources,³ etc. For most of these applications, the nature of the absorption process must be determined. As we know, the density scale length of the plasmas generated from the target surfaces can be estimated as⁴

$$L \equiv (\partial \ln n_e / \partial x)^{-1} \approx c_s \tau_p,$$

where $c_s = \sqrt{(ZT_e + T_i)/M_i}$ is the ion sound speed and τ_p is the pulse duration. For a pulse duration $\tau_p = 400$ fs, laser wavelength $\lambda_0 = 1.05 \mu\text{m}$, and electron temperature $T_e = 1$ keV, the scale length is $L \approx 0.057\lambda_0 \approx 0.4c/\omega_0$. In this case, collisional absorption is highly insufficient and resonance absorption at the critical surface is suggested to be one of the major absorption mechanisms.⁵

Resonance absorption is the collisionless absorption of p -polarized radiation in a plasma with a finite scale length. Some experiments^{6,7} show that it plays an important role even for plasmas with a scale length considerably shorter than the laser wavelength. However, to our knowledge, the previous theoretical works^{4,5} on resonance absorption are only valid for the case in which $L > \lambda_0$. For example, the classical Ginzburg function^{4,5,8} gives the peak value of the absorption at $(k_0L)^{1/3} \sin \theta_0 \approx 0.8$, but evaluating for the case

$k_0L = 0.5$ gives the optimum angle $\theta_{\text{opt}} \approx 90^\circ$, which is unphysical. Therefore, it is worthwhile to reexamine this absorption mechanism in a sharp density gradient plasma.

At higher laser intensity, say $L < v_{os}/\omega_0$, the electrons being pulled out and then returned to the plasma at the interface layer by the wave field can lead to a phenomenon like wave breaking. Thus, the electron plasma wave is hard to develop and vacuum heating⁹ tends to be dominant. Here, $v_{os} = eE_0/m_e\omega_0$ is the quiver velocity of the electron, E_0 is the electric field normal to the interface, and ω_0 is the laser frequency. A number of theoretical and numerical studies have added to this important mechanism.⁹⁻¹² However, this topic is still worthy of further investigation because there are still some points that the previous theoretical works do not solve.^{9,10} For example, why is the optimum angle about 45° ?¹¹ Furthermore, with a slightly surface expansion of scale length, the laser field would pull more electrons into the vacuum, and thus be even more strongly absorbed.¹¹ In this Brief Communication, a new detailed theoretical work for vacuum heating is also presented. It is found that the absorption rate increases with L as long as L does not significantly exceed the electron excursion length, and the optimum angle is independent of the laser intensity.

We consider a p -polarized plane electromagnetic wave incident at angle θ_0 onto a plasma slab with electron density $n_e(z)$. Without loss of generality, we take the electric vector in the x, z plane and the magnetic vector in \mathbf{e}_y . Hence the electromagnetic fields have the form

^{a)}Electronic mail: caihonb@yahoo.com.cn

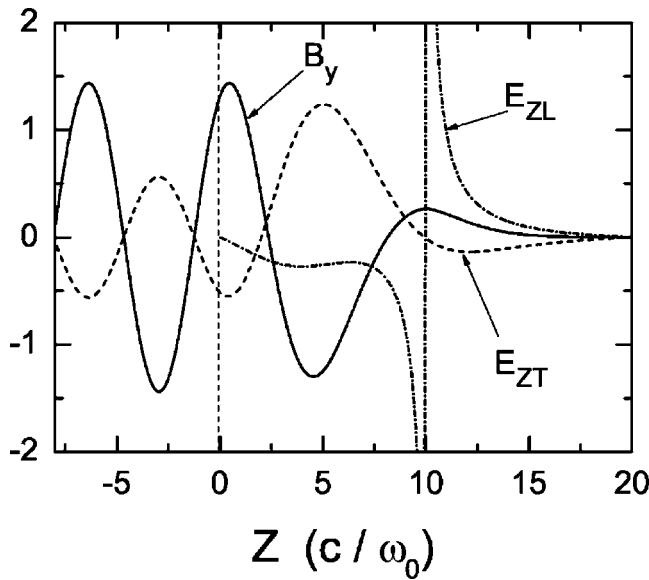


FIG. 1. The spatial profile of B_y , E_{zt} , and E_{zl} for $k_0L=10$ and $\theta_0=23^\circ$.

$$B_y(x, z, t) = B_y(z) \cdot e^{i\omega_0 t + ik_0 \sin \theta_0 x}, \quad (1)$$

where k_0 is the free-space wave number. We note that in the vacuum region ($z < 0$), the amplitude of the electromagnetic fields take this form, $B_y(z) = B_0(e^{ik_0 \cos \theta_0 z} + e^{-ik_0 \cos \theta_0 z + i\varphi})$. The first term is the incident laser wave, and the second term describes the reflected plane wave. It should be stressed that $\varphi = \varphi_r + i\varphi_i$. The real part denotes the phase shift and the imaginary part determines the damping of the reflected wave.⁴ From Maxwell's equations, we can get an equation for the magnetic field B_y easily,

$$\frac{d^2 B_y(z)}{dz^2} - \frac{1}{\varepsilon_1} \frac{d\varepsilon_1}{dz} \frac{dB_y(z)}{dz} + k_0^2 (\varepsilon_1 - \sin^2 \theta_0) B_y(z) = 0, \quad (2)$$

where ε_1 is the dielectric function. For a cold plasma, $\varepsilon_1(z) \approx 1 - \omega_{pe}^2(z)/\omega_0^2(1 + i\nu/\omega_0)$, where $\omega_{pe} = (4\pi n_e e^2/m_e)^{1/2}$ is the electron plasma frequency. ν is a small effective damping rate ($\nu/\omega_0 \ll 1$). The boundary conditions for Eq. (2) are freely outgoing waves at the vacuum side and evanescent waves at the high-density side. Therefore, by assuming that the plasma density is a linear function of position $n_e = n_{cr} \cdot z/L$ from 0 to $z = LN$, followed by a plateau at density Nn_{cr} (here $n_{cr} = m_e \omega_0^2 / 4\pi e^2$ is the critical density and $N = 15$), Eq. (2) can be solved numerically.

On the other hand, $E_z = -\partial_t A_z / c - \partial_z \phi$, where A_z is the vector potential and ϕ is the scalar potential. Therefore, we can separate the electric field into two parts: $E_z = E_{zt} + E_{zl}$, where $E_{zt} = -\partial_t A_z / c$ is the electromagnetic component associated with the incident laser wave while $E_{zl} = -\partial_z \phi$ is the electrostatic component associated with an electron plasma wave. It is important to stress that in the present question the latter is dominant since the electric field can drive a large plasma wave at the turning point resonantly. Starting from $\mathbf{B} = \nabla \times \mathbf{A}$, $\nabla \cdot \mathbf{A} = 0$, and $E_{zt} = -\partial_t A_z / c$, we obtain

$$\frac{d^2 E_{zt}}{dz^2} - k_0^2 \sin^2 \theta_0 E_{zt} = -k_0^2 \sin \theta_0 B_y. \quad (3)$$

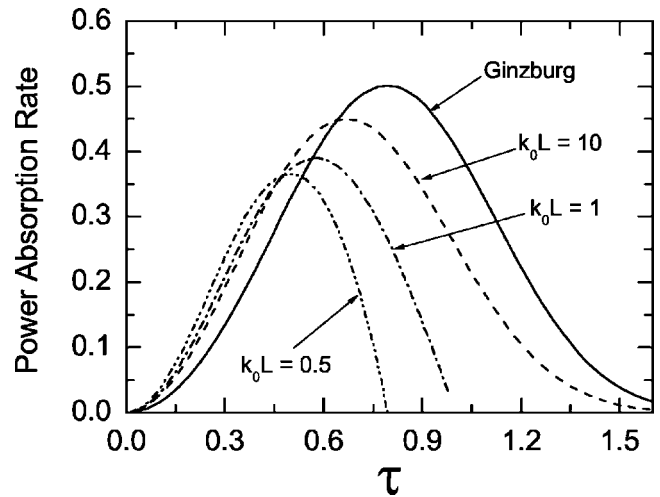


FIG. 2. The power absorption rate as a function of τ .

Here B_y is given by Eq. (2). Together with the boundary conditions, E_{zt} can be solved from Eq. (3). Combining Eq. (1) and Ampere's law, we have $E_z = \sin \theta_0 B_y / \varepsilon_1(z)$. Therefore, we obtain the absorption rate f_{RA} due to the damping of the plasma wave E_{zt} ,

$$f_{RA} = \frac{\nu}{8\pi I_L} \int_{-\infty}^{\infty} |E_{zt}|^2 dz, \quad (4)$$

where $I_L = cE_L^2/8\pi$ is the incident power. Physically, an electron plasma wave is resonantly excited near the critical density. When this plasma wave is damped, the energy is transferred to the plasma. From this point, our new model more precisely emphasizes the physics of resonance absorption and captures its basic features. It should be mentioned that as long as the damping rate ν is controlled within a certain range ($\nu < 0.05\omega_0$), the fractional energy absorbed is nearly independent of this damping rate. The reason is that the electrostatic component E_{zl} is negatively related to ν : as the damping becomes larger, the plasma wave develops more difficultly.

Equations (2) and (3) have been solved numerically. The spatial variations of the electromagnetic fields B_y , E_{zt} , and E_{zl} are plotted in Fig. 1. The absorption is caused by the nonzero wave field E_{zt} , which resonantly drives a large plasma wave (E_{zl}) with frequency ω_0 . The classical fractional absorption^{4,5,8} dependent on $\tau [\tau = (k_0L)^{1/3} \sin \theta_0]$ for $k_0L \geq 10$ is reproduced; see Fig. 2. However, as the scale length is reduced below $k_0L < 10$, the absorption peaks at smaller τ .

Here we compare our numerical results and the classical results in detail; see Fig. 3(a). In a large scale length ($k_0L \geq 10$) plasma, our numerical results are in good agreement with the classical results,⁴ satisfying $(k_0L)^{1/3} \sin \theta_0 \approx 0.8$. But in a sharp density gradient ($k_0L \leq 1$), the numerical results strongly disagree with the classical results, which are unsuitable in this region. Figure 3(b) shows more clearly under the logarithm coordinate. We can easily see that the optimum angle is still about 45° when $k_0L \approx 0.1 (L \approx 0.016\lambda_0)$ in our results, while it is greater than 90° when $k_0L \leq 0.5$ in the classical theory. Fitting the numerical results, we obtain

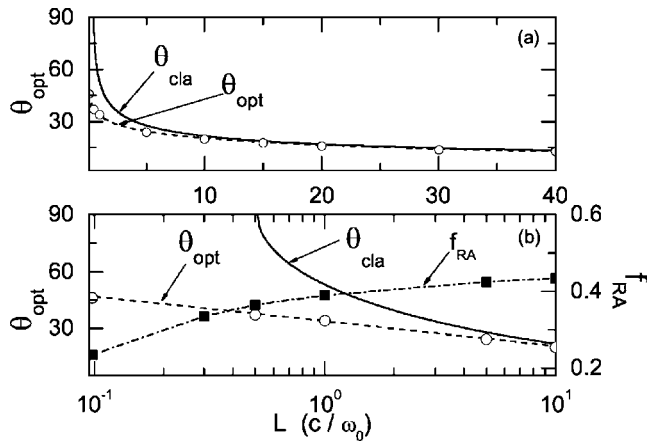


FIG. 3. The optimum angle and the power absorption rate as a function of L . The solid lines are for the classical results $(k_0L)^{1/3} \sin \theta_0 \approx 0.8$, the circles are for our numerical results of the optimum angle, the squares are for the fractional absorption, and the dashed lines and the dash-dotted line are for the fitting curves of the optimum angle and the fractional absorption, separately.

$$[(k_0L)^{0.6} + 1.97](\sin \theta_0 - 0.09) = 1.42. \quad (5)$$

The squares in Fig. 3(b) are the peak power absorption rate under a different scale length. We can see that the power absorption rate decreases with the decreasing of the scale length. Note that the minimum scale length we consider for resonance absorption is $k_0L=0.1$, but at higher laser intensity, resulting in $L \leq v_{os}/\omega_0$, vacuum heating will play a more important role.^{6,9-12}

Vacuum heating is an effect related to the classical resonance absorption¹² in that the laser electric field drives the electrons across a density gradient. An important difference between them is that in the latter process, the scale length is long enough; the electric field can resonantly excite a large electrostatic plasma wave at the critical point. In vacuum heating, on the other hand, the density gradient scale length is much smaller ($L < v_{os}/\omega_0$), so that no such resonance exists, and the electron motion is mainly driven by the electric field of the laser. In fact, the wave breaking phenomenon occurs within about one laser period,^{9,10} so the electrostatic wave is hard to develop. Therefore, the electromagnetic component is dominant, i.e., $u \gg v$. Here $u = eA_z/mc$ is the velocity associated with the electromagnetic component while $v = e\partial_z\phi/m\omega_0$ is the velocity associated with the electrostatic component. Therefore, we can safely neglect the electrostatic component in the wave equation for the laser radiation. In order to compare vacuum heating with resonance absorption in a small-scale-length plasma, we use the same model as mentioned above. From Maxwell's equations, we have the equation for the longitudinal part (parallel to \mathbf{e}_z) of the laser radiation,

$$\frac{d^2 A_z}{dz^2} + k_0^2(\epsilon_1 - \sin^2 \theta_0)A_z = 0, \quad (6)$$

where $\epsilon_1 = 1 - \omega_{pe}^2/\omega_0^2$ and the density profile is of the type $n_e = n_{cr} \cdot z/L$ from 0 to $z=LN$, followed by a plateau at density Nn_{cr} . Therefore, there are three different regions in this model: (i) vacuum, (ii) linear density layer, and (iii) plateau.

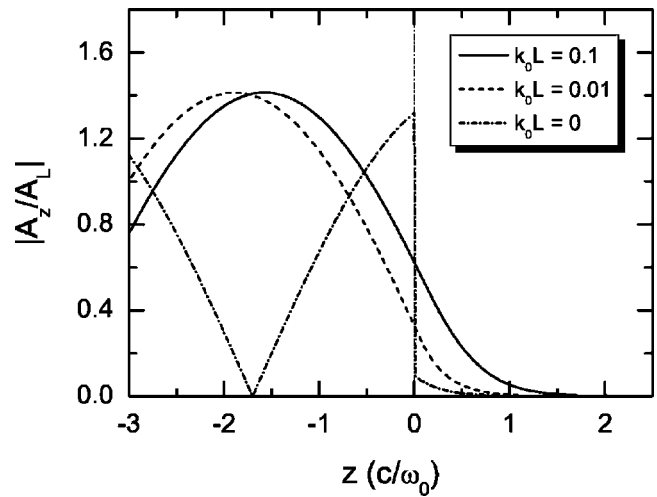


FIG. 4. The spatial profile of a_z for different plasma scale length. Three density profiles are considered: $N=15$ with $k_0L=0.1, 0.01$, and 0 [$k_0L=0$ corresponds to the step function model discussed by Kato *et al.* (Ref. 10)].

The solutions of Eq. (6) are (i) $A_z = A_0 \sin \theta_0 \sin(k_0 \cos \theta_0 z + \varphi)$, (ii) $A_z = A_0[\alpha \text{Ai}(\eta) + \beta \text{Bi}(\eta)]$, and (iii) $A_z = \alpha' \exp(-\kappa k_0 z)$, separately. Here $\eta = (\omega_0^2/c^2L)^{1/3}(z - L \cos^2 \theta_0)$ and $\kappa = \sqrt{N - \cos^2 \theta_0}$ are used, and $\text{Ai}(\eta)$ and $\text{Bi}(\eta)$ are the well-documented Airy functions. With the knowledge of the theory of classical electrodynamics, we know that the boundary conditions are $\mathbf{e}_z \times (\mathbf{B} - \mathbf{B}') = 0$ and $\mathbf{e}_z \times (\mathbf{E} - \mathbf{E}') = 0$. The electromagnetic fields are obtained from Maxwell's equations, $E_x = (\omega_0/k_0 \sin \theta_0) \partial_z A_z$, $B_y = -(ik_0/\sin \theta_0) \epsilon_1 A_z$, $E_z = -i\omega_0 A_z$. Therefore, the boundary conditions give the unknown constants, $\alpha = \sin \theta_0 / \sqrt{[\text{Ai}(\eta_0) + c_1 \text{Bi}(\eta_0)]^2 - [\text{Ai}'(\eta_0) + c_1 \text{Bi}'(\eta_0)]^2 / \eta_0}$, $\beta = c_1 \alpha$, where $c_1 = -[\kappa(k_0L)^{1/3} \text{Ai}(\eta_1) + \text{Ai}'(\eta_1)] / [\kappa(k_0L)^{1/3} \text{Bi}(\eta_1) + \text{Bi}'(\eta_1)]$ and $\eta_0 = \eta|_{z=0}$, $\eta_1 = \eta|_{z=NL}$.

It is important to stress that, in the limit $L=0$, our model recovers the step function model discussed by Kato *et al.*¹⁰ The spatial variation of A_z is plotted in Fig. 4. We can see

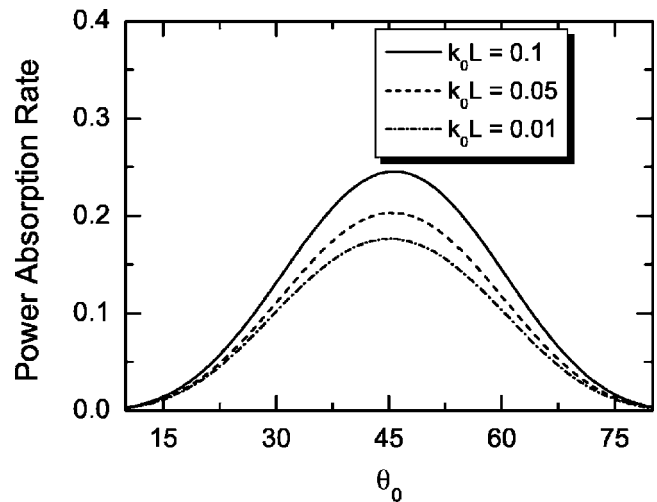


FIG. 5. The power absorption rate as a function of the incident angle for $I_L \lambda_0^2 = 1 \times 10^{17} \text{ W } \mu\text{m}^2/\text{cm}^2$.

that $A_z(0^+)$ decreases with the decreasing of the scale length. When $L=0$, a discontinuous point appears at $z=0$.

As we know, in such a sharp density gradient, the electromagnetic fields drop rapidly into the plasma; see Fig. 4. Therefore, only the electrons in the skin layer (the absorption layer) make a contribution to the absorption.¹⁰ According to Gibbon's theory,¹¹ the thickness of the absorption layer z_d can be defined as the effective excursion length of the electron at the interface, $z_d=2u_l/\omega_0$, where $u_l=(eA_0/m_e c) \times [\alpha \text{Ai}(\eta_0) + \beta \text{Bi}(\eta_0)]$. Notice that the thickness of the linear

density layer is $D_L=LN$. Therefore, in such a linear density profile with a plateau, the number of electrons in the absorption layer can be obtained by $N_a=\int_0^{z_d} n_e(z) dz$. If $L \geq z_d/N$, we obtain $N_a=z_d^2 n_{cr}/2L$; if the scale length is much shorter, $L < z_d/N$, we obtain $N_a=N n_{cr} z_d - LN^2 n_{cr}/2$. Thus, the energy absorbed from the laser light by the electrons is just $W_{\text{abs}}=(1/2)m_e u_l^2 N_a$ so that the power absorbed, per unit area, is just given as $dW_{\text{abs}}/dt \approx (1/2)\omega_0 m_e u_l^2 N_a$.¹² It is also equal to the fraction of power, $f_{\text{VH}}=I_{\text{abs}}/I_L$, lost from the electromagnetic wave, i.e.,

$$f_{\text{VH}} = \begin{cases} 8\alpha_0^2 [\alpha \text{Ai}(\eta_0) + \beta \text{Bi}(\eta_0)]^4 / k_0 L, & L \geq z_d/L, \\ 4[\alpha \text{Ai}(\eta_0) + \beta \text{Bi}(\eta_0)]^2 \{2\alpha_0 N [\alpha \text{Ai}(\eta_0) + \beta \text{Bi}(\eta_0)] - k_0 LN^2/2\}, & L < z_d/L. \end{cases} \quad (7)$$

Here $\alpha_0=eA_0/m_e c^2$ is the normalized amplitude of the vector potential. In the overdense region, the density can be as high as tens of critical density, therefore $L \geq z_d/N$ is satisfied in the range of the scale length in which we are interested here ($0.01 < k_0 L < 0.1$). Note that as long as $NL > 0.1 k_0^{-1}$ (e.g., $k_0 L > 0.01$ when $N \geq 10$), we have $\beta=0$. Therefore, in such a case, the optimum angle θ_{opt} can be obtained by $\partial f_{\text{VH}}/\partial \theta_0=0$, i.e.,

$$\text{Ai}(\tilde{\eta}_0) + 2\tilde{\tau}^2 \text{Ai}'(\tilde{\eta}_0) = \frac{\tilde{\tau}^2}{\tilde{\eta}_0^2 \Phi^2(\tilde{\eta}_0)} \text{Ai}(\tilde{\eta}_0) \text{Ai}'^2(\tilde{\eta}_0). \quad (8)$$

Equation (8) describes the relationship between θ_{opt} and L since $\tilde{\eta}_0=-L^{2/3} \cos^2 \theta_{\text{opt}}$ and $\tilde{\tau}=L^{1/3} \sin \theta_{\text{opt}}$. Notice that θ_{opt} is independent of the amplitude of the incident laser. In the nonrelativistic regime, $\theta_{\text{opt}} \approx 45^\circ$, consistent with the experimental^{13,14} and simulation results.¹¹ The absorption rate is sensitive to the scale length and incident angle; see Fig. 5. It is found that the power absorption rate increases with L as long as $L \leq v_{os}/\omega_0$, a result that agrees with Gibbon's simulation.¹¹ It is also found that the power absorption rate reaches as high as 25% when $k_0 L \approx 0.1$.

In conclusion, in a sharp density gradient, absorption mechanisms, including resonance absorption and vacuum heating, are investigated theoretically in order to explore the interaction of femtosecond laser pulses with solid targets. It is found that in the intensity regime from 10^{15} to 10^{17} W $\mu\text{m}^2/\text{cm}^2$, resonance absorption dominates when the scale length $k_0 L > 0.1$ while vacuum heating dominates when $k_0 L \leq 0.1$. It is also found that when $k_0 L \approx 0.1$, both resonance absorption and vacuum heating peak around

45° . Furthermore, we have found that the absorption rate due to vacuum heating increases with L as long as $L \leq v_{os}/\omega_0$.

This work was supported in part by the National Hi-Tech Inertial Confinement Fusion (ICF) Committee of China, National Science Foundation of China (NSFC) Grants No. 10135010, No. 10375011, No. 10335020/A0506, No. 10474081, and No. 10576035, the Natural Science Foundation of Shanghai (Project 05ZR14159), the Special Funds for Major State Basic Research Projects of China, and the Science Foundation of CAEP. One of the authors (Z.Y.C.) would like to thank the Bilateral project between Flanders and China.

¹M. Tabak, J. Hammer, M. E. Glinsky *et al.*, Phys. Plasmas **1**, 1626 (1994).

²A. Modena, Z. Najmudin, A. E. Dangor *et al.*, Nature (London) **377**, 606 (1995), and references therein.

³M. M. Murnane, H. C. Kapteyn, M. D. Rosen, and R. W. Falcone, Science **251**, 531 (1991).

⁴W. L. Kruer, *Physics of Laser Plasma Interactions* (Addison-Wesley, New York, 1988).

⁵V. L. Ginzburg, *The Properties of Electromagnetic Waves in Plasma* (Pergamon, New York, 1964).

⁶M. K. Grimes, A. R. Rundquist, Y. S. Lee, and M. C. Downer, Phys. Rev. Lett. **82**, 4010 (1999).

⁷J. C. Kieffer, P. Audebert, M. Chaker *et al.*, Phys. Rev. Lett. **62**, 760 (1989).

⁸W. Yu and J. Zhang, Opt. Commun. **134**, 91 (1997).

⁹F. Brunel, Phys. Rev. Lett. **59**, 52 (1987); Phys. Fluids **31**, 2714 (1988).

¹⁰S. Kato, B. Bhattacharyya, A. Nishiguchi, and K. Mima, Phys. Fluids B **5**, 564 (1993).

¹¹P. Gibbon and A. R. Bell, Phys. Rev. Lett. **68**, 1535 (1992); P. Gibbon, *ibid.* **73**, 664 (1994).

¹²S. C. Wilks and W. L. Kruer, IEEE J. Quantum Electron. **33**, 1954 (1997).

¹³Q. L. Dong, J. Zhang, and H. Teng, Phys. Rev. E **64**, 026411 (2001).

¹⁴L. M. Chen, J. Zhang, Q. L. Dong *et al.*, Phys. Plasmas **8**, 2925 (2001).